Low Cycle Fatigue Behaviour of Low Alloy Steels in High Temperature Pressurized Water

Norio Nagata, Shunji Sato, Yasuyuki Katada
National Research Institute for Metals, Tokyo, Japan

INTRODUCTION

Only a few papers have so far been reported on fatigue behaviour of LWR materials under simulated reactor coolant environments due to the experimental difficulties. Iida et al.(1986) reported systematic researches on the low cycle fatigue properties of carbon steels and low alloy steels in simulated LWR environments and proposed the life prediction equations. Terrell(1988) has recently reported the fatigue properties of carbon steel in a simulated PWR water environment. It was revealed that fatigue lives of ferritic steels under high temperature water decreased compared to those in ambient air, and depend not only on mechanical factors but also on environmental factors. The present report deals with low cycle fatigue tests conducted on low alloy steels for nuclear reactor pressure vessels in order to elucidate the corrosion fatigue behaviour of the materials in high temperature pressurized water. A crack initiation mechanism is also discussed.

MATERIALS AND EXPERIMENTAL PROCEDURE

Materials

Two types of low alloy steels, a forged steel equivalent to ASTM A508 cl. 3(specified as JIS SFVQ1A) and a rolled steel equivalent to ASTM A533B cl. 1(JIS SQV2A) were employed. Round bar specimens with test sections of 8mm in diameter and 16mm in length having projections for strain measurement were used. Specimen axes were parallel or perpendicular to the forging direction or the rolling direction.

Table 1 Chemical compositions of low alloy steels tested.(wt%)

	C	Si	Mn	P	S	Ni	Cr	Mo	V	Cu
A508 cl.3	0.17	0.28	1.38	0.003	0.003	0.74	0.15	0.48	0.003	
A533B cl.1	0.19	0.24	1.28	0.008	0.007	0.64	0.19	0.45	tr.	0.04

Apparatus

An apparatus for fatigue tests in high temperature pressurized water consists of an electro servo-hydraulic fatigue testing machine of a capacity of ±49kN, an austenitic stainless steel autoclave of a capacity of 6L for the maximum operating condition of 573K in temperature and 9.8MPa in pressure, and a test water recirculation system of a flow rate of 30L/h. Water chemistry was monitored successively for dissolved oxygen(DO) concentration, pH and conductivity. The axial strain of the specimen was controlled by monitoring the difference of outputs of a couple of DTFs, of which cores were connected to the jigs on the projections of the specimen.

Test Condition

Low cycle fatigue tests were conducted under a fully reversed triangular wave form at various strain rates. Test environments were pure water at 561K and 7.8MPa, containing DO ranging from 10ppb to 8000ppb including the BWR condition. In addition, fatigue tests in air at room temperature or 561K were performed for comparison.

EXPERIMENTAL RESULTS

Low Cycle Fatigue Properties at Room Temperature

First, S-N curves at room temperature were obtained for the basis of the evaluation of environmental effect on the low cycle fatigue properties of the low alloy steels. No relations between the specimen axes and the fatigue properties were observed so that the data for the specimens with different orientations were analyzed as single group data. Data for both steels at strain rate of 0.1%/s are plotted in Fig. 1. Since the total strain range, $\Delta\varepsilon_t$ consists of the elastic strain component, $\Delta\varepsilon_e$ and the plastic strain component, $\varepsilon\Delta_p$, and each component exhibits a good linear relation to the fatigue life as seen in the figure, $\Delta\varepsilon_t$ can be expressed as

$$\Delta\varepsilon_t = \Delta\varepsilon_e + \Delta\varepsilon_p = AN_{25}^{-\alpha} + BN_{25}^{-\beta} \qquad (1)$$

where A, B, α and β are constants, and N_{25} is a number of cycles at which the tensile stress amplitude decreases to 75% of the amplitude at half of the fatigue life. Regression curves of S-N data for two steels obtained by eq. 1 are also shown in Fig. 1. It is seen that the curves at room temperature show similar trends implying no difference in cyclic load responses of both steels.

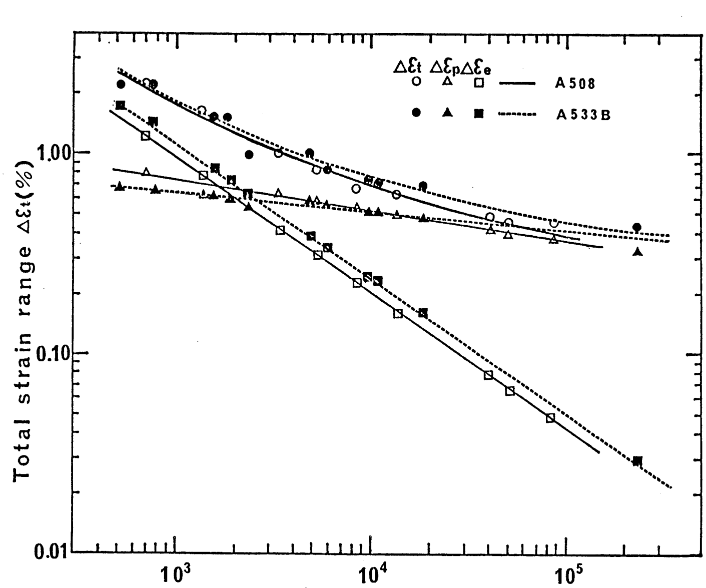

Fig. 1 Data of $\Delta\varepsilon_t$, $\Delta\varepsilon_e$, $\Delta\varepsilon_p$ vs N_{25} and the fitting curves by Eq. 1 for A508 and A533B steels in ambient air.

Low Cycle Fatigue Properties at High Temperature

Low cycle fatigue tests in water at 561K containing 100ppb DO simulated to the BWR water environment and in high temperature air were conducted. Results obtained at strain rate of 0.1%/s are shown in Fig. 2, in which the data at room temperature are also shown for comparison. It is apparent that fatigue lives of A508 steel in water and in air at high temperature are nearly same or rather longer at lower total strain ranges compared to those in ambient air, while these fatigue lives of A533B steel become shorter than those in ambient air at high total strain ranges. Since the fatigue lives for both steels in water and in air at high temperature show similar trends and reductions of fatigue lives in water due to the environmental degradation are found, it can be said that fatigue properties in high temperature water are governed by the factors of temperature and water environment. It seems that the trend that at lower total strain ranges the fatigue lives at high temperature are rather longer than those at room temperature might be due to dynamic strain aging(Iida et al, 1986, Terrell 1988).

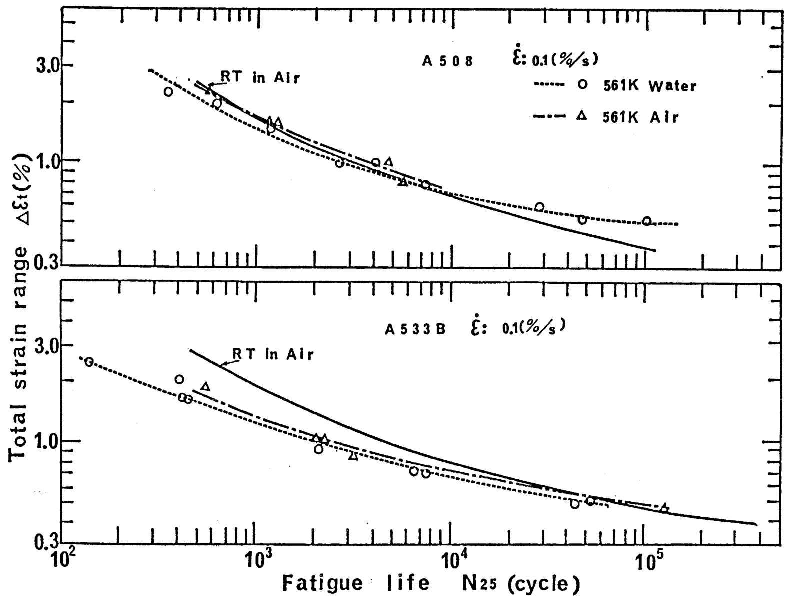

Fig. 2 Comparison of $\Delta\varepsilon_t$ vs N_{25} curves for ambient air, 561K air and high temperature water.

S-N curves at strain rates of 0.1%/s, 0.01%/s and 0.001%/s for both steels in high temperature water are shown in Fig. 3. It is seen that A533B steel shows a distinct strain rate dependence of fatigue life compared to that of A533B steel.

Effect of Dissolved Oxygen

DO concentration dependence of fatigue life in high temperature water obtained under the conditions of total strain range of about 0.8%, strain rate of 0.1%/s and DO concentration ranging from 10ppb to 8000ppb is shown in Fig. 4. It is apparent that both steels show a similar DO dependence, that is, little changes of fatigue lives at DO concentrations below 200ppb, while they decreased with increasing DO concentration and above 1000ppb down to half to one third of those at lower DO concentrations. Similar transition behaviour was also reported for low alloy steel and carbon steel(Iida et al, 1986).

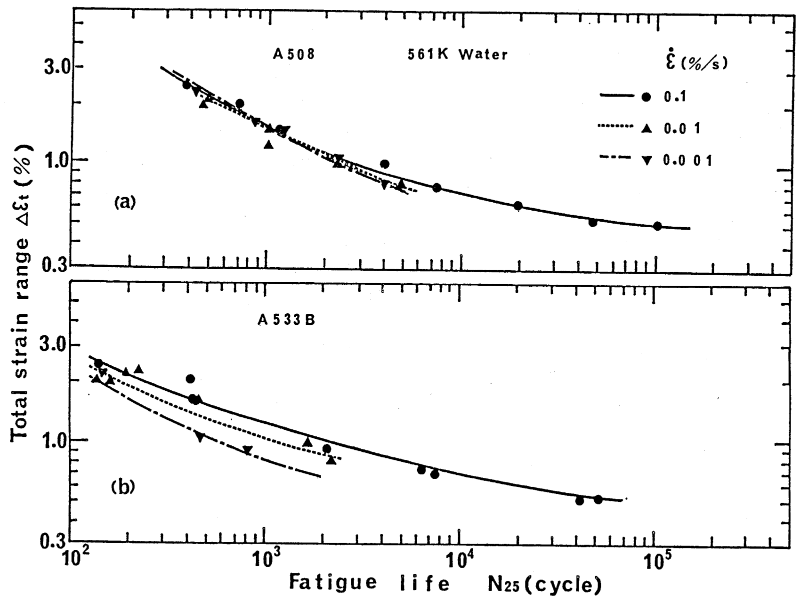

Fig. 3 S-N curves at various strain rates for A508 and A533B steels in high temperature water.

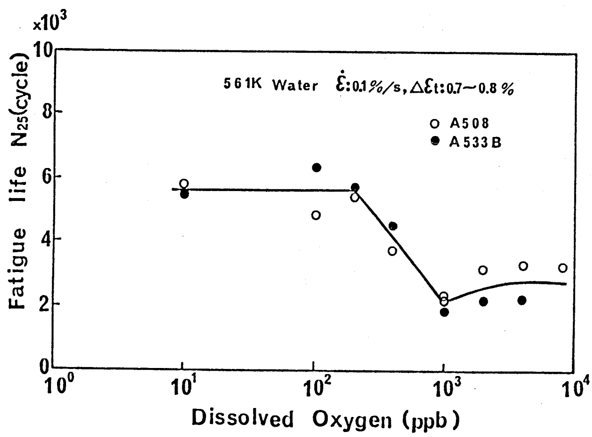

Fig. 4 DO dependence of N_{25} for A508 and A533B steels at high temperature.

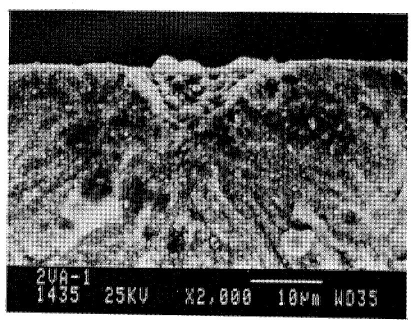

Photo. 1 An example of crack initiations of A533B in high temperature water. ($\Delta\varepsilon_t$ = 1.0%, $\dot{\varepsilon}$ =0.1%/s)

Fractography

Cracked surfaces of the specimens after the low cycle fatigue tests in high temperature water were observed by a SEM. Photo. 1 shows a typical example of crack initiations at small dimples considered as corrosion pits. It is seen that the crack initiates at the bottom of the dimple and propagates leaving a quasi-brittle fracture region followed by ductile striations. The size of the dimple is of the order of 10 μm that is the same order of MnS inclusions in the matrix. No cracks with such dimples were observed on the specimens tested in high temperature air or ambient air.

DISCUSSION

MnS Inclusion and Crack Initiation

Present results showed that low cycle fatigue properties of A508 steel and A533B steel in high temperature water are essentially same except the strain rate dependence. Both steels, one is forged and the other rolled, are quite similar in terms of chemical composition, microstructure and mechanical property. However, they are different in terms of content of impurity such as sulphur and phosphorus. A533B steel contains more than twice of these impurities in A508 steel. It is known that fatigue crack growth behaviour of ferritic steels in high temperature water depends strongly on their sulphur contents, namely, little acceleration of crack growth is observed on the steels containing sulphur impurity below 0.010wt%, above which concentrations, on the other hand, crack growth is accelerated markedly(Atkinson et al, Van Der Sluys et al, 1986). Based on these knowledges the difference of sulphur contents in the present steels seems to be insignificant. In order to see the susceptibility to the corrosion fatigue, correlations between fatigue life and density of corrosion pits which were observed at the test sections of the specimens were investigated. Since the frequency of corrosion pit generation did not depend on total strain range, relations between the average density of corrosion pits and strain rate were surveyed as shown in Fig. 5. From the comparison of scatter bands of the density of pits for both steels, it is seen that the density of pits increases with decreasing strain rate, in other word, it correlates with immersing time in the environment. Furthermore, it is apparent that the density of pits observed is higher for A533B steel than for A508 steel in a range of strain rate tested. This coincides with the fact that strain rate dependence of fatigue life was stronger for A533B steel than for A508 steel as already shown in Fig. 3. Therefore, it can be concluded from the abovementioned that as for the fatigue damage mechanism of low alloy steels in high temperature water fatigue cracks initiate at corrosion pits generated by dissolution of MnS inclusions located on the material surface, and furthermore, the crack initiation process should be more sensitive to sulphur content of the steel than the crack propagation process is.

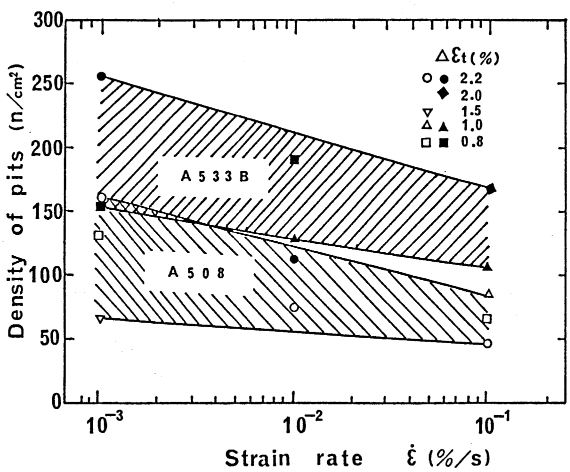

Fig. 5 Relation between density of pits and strain rate.

Comparison with ASME Code Sec.Ⅲ

A comparison of the present data expressed as pseudo-stress with ASME Boiler & Pressure Vessel Code Sec.Ⅲ design fatigue curves(ASME, 1986) is shown in Fig. 6. It is seen that all the data in high temperature water locate above the design curves and there are margins of twice in stress and ten times in fatigue life for

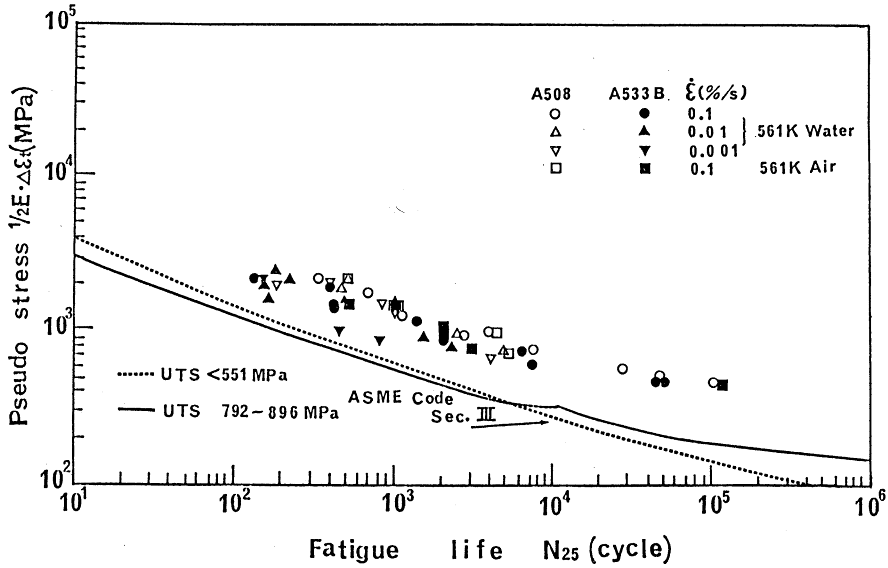

Fig. 6 Comparison of present data to the design fatigue curves of ASME Code Sec.Ⅲ.

the data at strain rate of 0.1%/s. Although the strain rate dependence of fatigue life for A533B steel is stronger than that for A508 steel as aforementioned, it can be concluded that both steels possess a safety margin in reactor coolant environment.

CONCLUSIONS

1)Reduction of fatigue lives of low alloy steels in high temperature water in comparison with those in ambient air were observed. However, it decreased with decreasing total strain range. In the case of A508 steel at low strain ranges, the fatigue lives in high temperature water were rather longer than those at ambient air.

2)A533B steel showed a distinct strain rate dependence in high temperature water compared to A508 steel.

3)Both steels showed a similar dependence of DO concentration with a transition of fatigue life reduction at the range from 200ppb to 1000ppb.

4)Fatigue cracks initiated at corrosion pits generated by dissolution of MnS inclusions at the surface of the material and fatigue lives decreased with increasing the density of corrosion pits.

5)The crack initiation process would be more sensitive to the sulphur content of steels than the crack propagation process is.

6)In comparison with the design fatigue curves of ASME Boiler and Pressure Vessel Code Sec. Ⅲ, it was concluded that the low alloy steels tested possess a safety margin to the integrity even in high temperature water environment.

REFERENCES

ASME, (1986). Boiler & Pressure Vessel Code Sec.Ⅲ.

Atkinson, J. D. and Forrest, J. E. (1986). Proc. 2nd IAEA Specialists' Meeting on Subcritical Crack Growth, NUREG/CP-0067, Vol. 2, pp.153-178.

Iida, K. Kobayashi, H. and Higuchi, M. (1986). ibid. Vol. 2, pp.385-409.

Terrell, J. B. (1988). J. Mater. Eng. Vol.10, pp.193-203.

Van Der Sluys, W. A. and Emanuelson, R. H. (1986). Proc. 2nd IAEA specialists' Meeting on Subcritical Crack Growth, NUREG/CP-0067, Vol. 1, pp.199-218.